Enhancing 2D elasticity and viscosity images: A denoising approach for reflected and random noise removal

Mejora de imágenes 2D de elasticidad y viscosidad: un enfoque de eliminación de ruido para la eliminación de ruido reflejado y aleatorio

Aprimorando imagens 2D de elasticidade e viscosidade: uma abordagem de redução de ruído para remoção de ruído refletido e aleatório

Nguyen Sy Hiep[1,2]
Duc-Nghia Tran[3]
Vijender Kumar Solanki[4]
Duc-Tan Tran[5]
Quang Hai Luong[6]

Received: May 5th, 2025
Accepted: July 16th, 2025
Available: September 5th, 2025

How to cite this article:
N. S. Hiep, D.-N. Tran, V. K. Solanki, D.-T. Tran, and Q. H. Luong, "Enhancing 2D elasticity and viscosity images: A denoising approach for reflected and random noise removal," *Revista Ingeniería Solidaria,* vol. 21, no. 3, 2025.
doi: https://doi.org/10.16925/2357-6014.2025.03.02

Research article. https://doi.org/10.16925/2357-6014.2025.03.02

[1] Graduate University Of Science And Technology, VAST, Ha Noi, Vietna,

[2] Thai Nguyen University of Information and Communication Technology, Thai Nguyen, Vietnam

[3] Institute of Information Technology, Vietnam Academy of Science and Technology, Hanoi, Vietnam

[4] Department of Computer Science and Enginnering, Stanley College Of Engineering & Technology For Women, Hyderabad, TG, INDIA

[5] Faculty of Electrical and Electronic Engineering, Phenikaa School of Engineering Phenikaa University, Hanoi, Vietnam

ORCID: https://orcid.org/0000-0002-7673-388X

[6] Department of Biomedical Engineering, Institute of Control Engineering Le Quy Don Technical University, Hanoi, Vietnam

ORCID: https://orcid.org/0009-0001-8860-4735

Corresponding Email: luonghai@lqdtu.edu.vn

Abstract

Introduction: Nowadays, Shear Wave Elastography (SWE) images are extensively employed for the early detection of various cancers including liver, breast, thyroid, and prostate cancers. This plays a pivotal role in cancer management. SWE images rely on estimating the Complex Shear Modulus (CSM), which is contingent upon two parameters of tissue properties in vivo: elasticity and viscosity.

Problem: Reflected noise, random noise, and speckle noise affect the quality of ultrasound images.

Objective: Simulating the shear wave propagation by using Finite-Difference Time-Domain (FDTD) method, removing noises, and reconstructing the elasticity and viscosity images of tissues.

Methodology: In this study, we utilized several noise filters to eradicate unwanted noise. We employed a directional filter to eliminate reflected noise, an LMS filter to remove random noise, and a median filter for speckle noise removal. Subsequently, we applied the AHI algorithm to estimate the elasticity and viscosity of tissue.

Results: The elasticity and viscosity 2D images are estimated, underwent filtering resulting in improved images quality. Root Mean Square Error (RMSE) was used to evaluate the effectiveness of the estimation.

Conclusion: The obtained results include 2D images of tissue elasticity and viscosity, demonstrating the effectiveness of the filter in noise removal and AHI algorithm in estimating.

Originality: We propose filters for noise removal (consist of reflected noise), before applying AHI algorithm to estimate elasticity and viscosity of tissue.

Limitation: The model is applied with a limited range of parameter values in the input scenario.

Keywords: Shear wave, Reflected noise, Directional filter, LMS filter, Median filter, AHI algorithm, Elastography image.

Resumen

Introducción: Actualmente, las imágenes de elastografía por ondas de corte (SWE) se utilizan ampliamente para la detección temprana de diversos tipos de cáncer, como el de hígado, mama, tiroides y próstata. Esto desempeña un papel fundamental en el tratamiento del cáncer. Las imágenes SWE se basan en la estimación del módulo de corte complejo (CSM), que depende de dos parámetros de las propiedades tisulares in vivo: elasticidad y viscosidad.

Problema: El ruido reflejado, el ruido aleatorio y el ruido de moteado afectan la calidad de las imágenes de ultrasonido.

Objetivo: Simular la propagación de ondas de corte mediante el método de diferencias finitas en el dominio del tiempo (FDTD), eliminando el ruido y reconstruyendo las imágenes de elasticidad y viscosidad de los tejidos.

Metodología: En este estudio, utilizamos varios filtros de ruido para eliminar el ruido no deseado. Se empleó un filtro direccional para eliminar el ruido reflejado, un filtro LMS para eliminar el ruido aleatorio y un filtro de mediana para eliminar el ruido de moteado. Posteriormente, se aplicó el algoritmo AHI para estimar la elasticidad y la viscosidad del tejido.

Resultados: Se estimaron imágenes 2D de elasticidad y viscosidad, las cuales se filtraron, lo que mejoró la calidad de las imágenes. Se utilizó el Error Cuadrático Medio (RMSE) para evaluar la efectividad de la estimación.

Conclusión: Los resultados obtenidos incluyen imágenes 2D de elasticidad y viscosidad tisular, lo que demuestra la efectividad del filtro en la eliminación de ruido y del algoritmo AHI en la estimación.

Originalidad: Se proponen filtros para la eliminación de ruido (consisten en ruido reflejado) antes de aplicar el algoritmo AHI para estimar la elasticidad y la viscosidad tisular.

Limitación: El modelo se aplica con un rango limitado de valores de parámetros en el escenario de entrada.

Palabras clave: Onda transversal, Ruido reflejado, Filtro direccional, Filtro LMS, Filtro de mediana, Algoritmo AHI, Imagen de elastografía.

Resumo

Introdução: Atualmente, as imagens de Elastografia por Ondas de Cisalhamento (SWE) são amplamente utilizadas para a detecção precoce de diversos tipos de câncer, incluindo câncer de fígado, mama, tireoide e próstata. Isso desempenha um papel fundamental no manejo do câncer. As imagens de SWE dependem da estimativa do Módulo de Cisalhamento Complexo (CSM), que é dependente de dois parâmetros das propriedades do tecido in vivo: elasticidade e viscosidade.

Problema: Ruído refletido, ruído aleatório e ruído de speckle afetam a qualidade das imagens de ultrassom.

Objetivo: Simular a propagação da onda de cisalhamento utilizando o método de Diferenças Finitas no Domínio do Tempo (FDTD), remover ruídos e reconstruir as imagens de elasticidade e viscosidade dos tecidos.

Metodologia: Neste estudo, utilizamos diversos filtros de ruído para eliminar ruídos indesejados. Empregamos um filtro direcional para eliminar o ruído refletido, um filtro LMS para remover o ruído aleatório e um filtro de mediana para remover o ruído de speckle. Posteriormente, aplicamos o algoritmo AHI para estimar a elasticidade e a viscosidade do tecido.

Resultados: As imagens 2D de elasticidade e viscosidade foram estimadas e submetidas a filtragem, resultando em melhoria na qualidade das imagens. O Erro Quadrático Médio (RMSE) foi utilizado para avaliar a eficácia da estimativa.

Conclusão: Os resultados obtidos incluem imagens 2D da elasticidade e viscosidade do tecido, demonstrando a eficácia do filtro na remoção de ruído e do algoritmo AHI na estimativa.

Originalidade: Propomos filtros para remoção de ruído (consistindo em ruído refletido) antes da aplicação do algoritmo AHI para estimar a elasticidade e a viscosidade do tecido.

Limitação: O modelo é aplicado com uma faixa limitada de valores de parâmetros no cenário de entrada.

Palavras-chave: Onda de cisalhamento, Ruído refletido, Filtro direcional, Filtro LMS, Filtro mediano, Algoritmo AHI, Imagem de elastografia.

I. INTRODUCTION

SWE imaging has become an important tool in the medical, especially in the early diagnosis of diseases, including cancer. This method aids healthcare professionals in detecting early signs of cancer. Additionally, it offers benefits such as low cost, non-invasiveness, and quick examination time. However, like any other medical methods, SWE image also has limitations, especially the quality of imaging is affected by noise.

Diseased tissue often exhibits distinct elasticity and viscosity values compared to healthy tissue, which makes accurately estimating these values crucial for distinguishing diseased tissue with normal tissue. This estimation is based on the analysis of shear wave velocity which propagate in tissue. In our research, we employed a

vibrating needle to generate these shear waves. Capturing this velocity signal necessitated the use of a Doppler ultrasound system. Before being captured by the ultrasound probe, the shear waves propagated through both normal tissue and diseased tissue (tumor). At the border between normal and diseased tissue, a part of the shear wave's energy was reflected back to the source, affecting the incident wave [1-3], while the rest of the energy continued to propagate through the diseased tissue. Moreover, the shear waves propagated through tissue is also affected by random noise [3].

In Section 2, the authors review previous studies related to SWE image and methods for noise removal. Section 3, we presents the background study. In Section 4 we have demonstrated the proposed methodology. Following that, Section 5 presents experimental results and discusses. Finally, In Section 6, the authors summarize the conclusions and propose the future works for this research.

2. LITERATURE REVIEW

The earlier cancer can be identified, the higher the chances for effective treatment. However, approximately 50% of cancers are diagnosed at an advanced stage [4-5], SWE image is highly useful for the early detection of malignant tumors. Research by Jung Min Chang et al. demonstrated a significant difference in stiffness between benign and malignant breast masses. The average elasticity values were significantly higher in malignant masses (153.3 kPa ± 58.1) compared to benign masses (46.1 kPa ± 42.9) [6]. Therefore, identifying tissue stiffness provides many benefits for diagnosis. However, noise in SWE images presents a significant challenge in signal processing. Removing it is crucial for improving the reliability of SWE images. Numerous studies aim to eliminate noise to enhance signal reliability.

In 2007, Zheng et al. utilized the Kalman filter to analyze the harmonic motion of particle velocities at different spatial locations [7]. Their method estimated both absolute phase and phase differences, allowing for the determination of shear wave speed and dispersion curves across various frequency bandwidths. However, their approach to reconstructing the Complex Shear Modulus was computationally intensive due to requiring multiple shear wave frequency measurements, which could potentially lead to artifacts. The authors did not address issues related to reflection noise and speckle noise in their study.

In the research [8], Hengzhao ***et al.*** determined the viscosity and elasticity of tissue by calculating the attenuation α_s of shear wave and velocity c_s. The source generated shear waves was a probe that created a non-focused ultrasound beam (4.1 MHz with 128 elements and 400s duration). Another probe was used to receive signals

was placed on the opposite side of the object, with μ_1 = 4kPa, μ_2 = 1Pa.s, and mass density of 1000 kg / m^3. The sampling frequency was 10 kHz. The values of c_s and α_s were calculated by 2D Fourier transform (K-space). Using both the peak extraction method and the full-width-at-half-maximum (FWHM) method. Viscosity and elasticity values are important factors in evaluating tissue properties. However, the authors of this study did not address the types of noise generated on their study, and the phantom study had consistent viscosity and elasticity. There was no scenario where a tumor needed to be tested.

In the study [2] of Deffieux T, an experiment was conducted to examine the effect of reflected waves on the estimation of shear wave velocity. The reflected waves were generated at the interface between two media with different stiffness levels and affect the incident wave, thereby reducing the signal quality. The authors conducted experiments on objects with different diameters and different stiffnesses (8 and 12mm), respectively, at 10, 15, and 20 kPa, with a background shear modulus of 5 kPa. The shear modulus maps obtained after estimating the shear wave velocity (using time-domain cross correlation) showed the effect of reflected noise on the quality of the shear modulus images. Deffieux T used a simple directional filter to remove reflected noise. The quality of the shear modulus image was improved significantly. However, this study did not mention random noise. This is also an unavoidable factor in the signal acquisition process.

In our previous study [3], The Finite-Difference Time-Domain (FDTD) method was employed to simulate the propagation of waves in tissue containing a tumor. Diseased tissue has higher elasticity and viscosity values than healthy tissue. Specifically, the elasticity and viscosity values of healthy tissue are 100 Pa and 0.1 Pa·s, respectively. The elasticity and viscosity values of the tumor tissue are 1300 Pa and 0.3 Pa·s, respectively. The density was 1000 kg/m³, and the frequency of needle vibration was 200 Hz. The amplitudes of the incident wave and the reflected wave were 2 mm and 0.4 mm, respectively. The sampling frequency was 2000 Hz. Directional and LMS filters were employed to remove both reflected and random noise [9]. The AHI algorithm was used to estimate SWE images of elasticity and viscosity based on velocity [3]. In this study, we introduce several improvements compared to previous work. Directional and LMS filters, along with a median filter, were employed to eliminate speckle noise [10-13]. 2D SWE images of elasticity and viscosity were estimated. To assess the effectiveness of the filtering method, the root mean square error (RMSE) was used. RMSE represents the average error between the estimated image and the ideal image. A smaller RMSE value indicates a better filtering method

[14-15]. Therefore, in addition to qualitative evaluation, the RMSE parameter serves as the basis for evaluating the effectiveness of the method in this research.

3. BACKGROUND STUDY

We employed the Finite Difference Time Domain (FDTD) method to simulate the propagation of shear waves. This method considers both spatial and temporal factors that affect shear wave velocity, allowing for a more realistic simulation compared to using the wave equation. To eliminate noise in the composite wave, we employed a directional filter and an LMS filter sequentially to remove both reflected and random noise. The AHI algorithm was utilized to estimate the elasticity and viscosity images based on the filtered velocity of the shear wave. Lastly, speckle noise in the elasticity and viscosity images was removed using a median filter.

3.1. Generation and propagation of shear wave

A needle is controlled to vibrate at a constant frequency on the surface of tissue, inducing compression and expansion of the tissue, thus generating shear waves. These shear waves propagate through the tissue and reach a tumor mass (Figure 1). The particle velocity of the shear wave attenuates spatially and varies as it travels through two different environments (healthy tissue and diseased tissue). This velocity signal is captured by a Doppler ultrasound system.

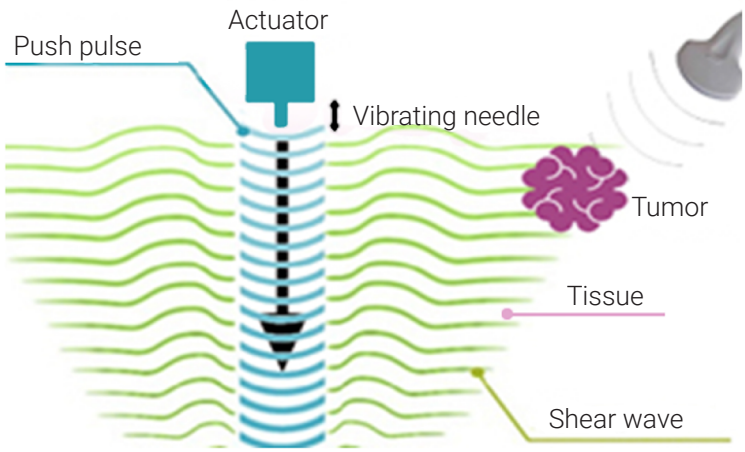

Figure 1. Vibrating needle generates shear wave [3].

e-ISSN 2357-6014 / Vol. 21, no. 3 / september-december 2025 / Bogotá D.C., Colombia
Universidad Cooperativa de Colombia

3.2. Complex Shear Modulus

The CSM $G\,(x,\ y,\omega)$ is defined as following equation (1).

$$G\left(x,y,\omega\right)=\mu(x,y)-i\omega\eta(x,y) \tag{1}$$

Where $\mu\ (x,\ y)\ (x,\ y)$ represents elasticity, and $\eta\ (x,\ y)$ represents viscosity at the spatial position

The CSM and the velocity of shear wave have relationship with each other through Equations (2), (3) and (4).

$$\rho\partial_t v_z=\partial_x\sigma_{zx}+\partial_y\sigma_{zy} \tag{2}$$

$$\partial_t\sigma_{zx}=(\mu+\eta\partial_t)\partial_x v_z \tag{3}$$

$$\partial_t\sigma_{zy}=(\mu+\eta\partial_t)\partial_y v_z \tag{4}$$

Where v_z is the particle velocity vector in the $(x,\ y)$ plane, σ_{zx}, σ_{zy} is element of the stress tensor, ρ is the density of the tissues, ∂_z represents a partial derivative operator with respect to time, denoted as t, ∂_x is partial derivative operator with respect to the spatial coordinate x, ∂_y represents a partial derivative operator with respect to the spatial coordinate y.

Applying the Finite-Difference Time-Domain (FDTD) method to transform Equations (2), (3) and (4) into Equations (5), (6) and (7) in discretized [10], [16].

$$v_z{}^{n+1}\big|_{i,j}=v_z{}^{n}\big|_{i,j}+\frac{\Delta_t}{\rho\Delta_x}\left(\sigma_{zx}{}^{n+\frac{1}{2}}\big|_{i+\frac{1}{2},j}-\sigma_{zx}{}^{n+\frac{1}{2}}\big|_{i-\frac{1}{2},j}\right) \tag{5}$$
$$+\frac{\Delta_t}{\rho\Delta_y}\left(\sigma_{zy}{}^{n+\frac{1}{2}}\big|_{i+\frac{1}{2},j}-\sigma_{zy}{}^{n+\frac{1}{2}}\big|_{i-\frac{1}{2},j}\right)$$

$$\sigma_{zx}{}^{n+1}\big|_{i+\frac{1}{2},j}=\sigma_{zx}{}^{n-\frac{1}{2}}\big|_{i+\frac{1}{2},j}+\frac{\mu\Delta_t}{\Delta_x}\left(v_z{}^{n+1}\big|_{i+1,j}-v_z{}^{n+1}\big|_{i,j}\right) \tag{6}$$
$$+\frac{\eta}{\Delta_x}\left(v_z{}^{n+1}\big|_{i+1,j}-v_z{}^{n+1}\big|_{i,j}\right)-\frac{\eta}{\Delta_x}\left(v_z{}^{n}\big|_{i+1,j}-v_z{}^{n}\big|_{i,j}\right)$$

$$\sigma_{zy}^{\,n+1}\Big|_{i+\frac{1}{2},j} = \sigma_{zx}^{\,n-\frac{1}{2}}\Big|_{i+\frac{1}{2},j} + \frac{\mu\Delta_t}{\Delta_y}\left(v_z^{\,n+1}\Big|_{i+1,j} - v_z^{\,n+1}\Big|_{i,j}\right) \tag{7}$$

$$+\frac{\eta}{\Delta_y}\left(v_z^{\,n+1}\Big|_{i+1,j} - v_z^{\,n+1}\Big|_{i,j}\right) - \frac{\eta}{\Delta_y}\left(v_z^{\,n}\Big|_{i+1,j} - v_z^{\,n}\Big|_{i,j}\right)$$

Δx and Δy represent the distances between consecutive spatial locations along the X-axis and Y-axis, respectively. Δt represents the sampling cycle or time step, i represents a spatial increment along the X-axis, j is spatial increment along the Y-axis, n represents a temporal step.

4. PROPOSED METHODOLOGY

The workflow diagram in Figure 2 outlines the data processing flow, providing a clear and comprehensive overview of the sequence of signal processing steps in this paper.

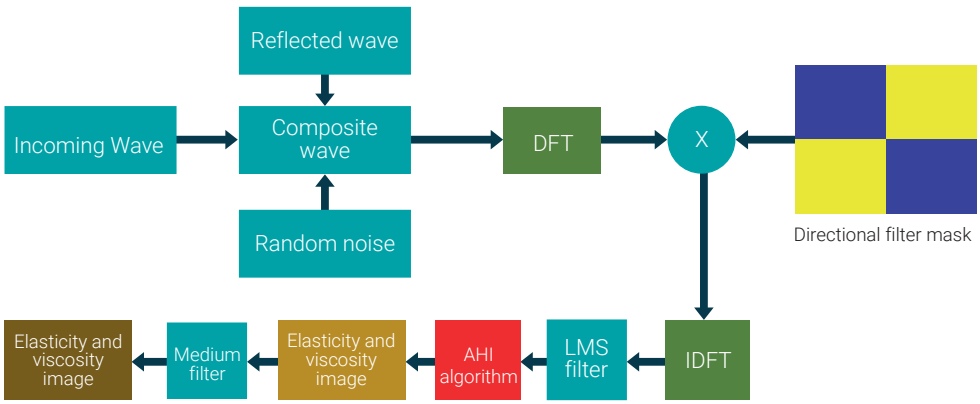

Figure 2. Data processing flow of the proposed method.
Reference: The authors

The measured - shear wave velocity signal contained reflected and random noise. This signal underwent discrete Fourier transformation. (DFT), then multiplied by a directional filter mask to eliminate the reflected noise in the composite wave. Subsequently, the velocity signal was inverse discrete Fourier transformed (IDFT). The velocity signal then underwent a Least Mean Squares (LMS) filter to remove random noise before proceeding with the estimation of elasticity and viscosity by using the

AHI algorithm. The estimated-elasticity and viscosity images were passed through a median filter to smooth images.

4.1. Eliminating Reflection Noise by using Directional Filter

In this study, to eliminate reflected noise, we utilized a directional filter by multiplying the composite signal after Fourier transformation with a directional filter mask (Figure 3). This mask allowed selected signals to pass through while blocking the remaining signals. The directional filter mask in Figure 3 was encoded with two colors: dark blue and yellow. The dark blue color represents a value of 0, blocking the signal from passing through, while the yellow color represents a value of 1, allowing the signal to pass through.

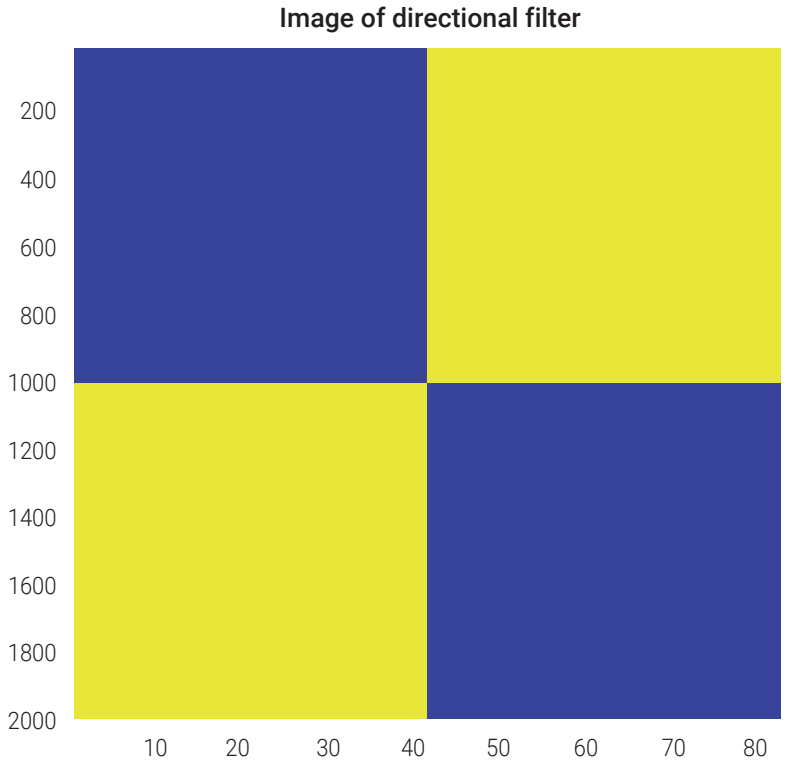

Figure 3. Image of the directional filter mask.
Reference: The authors

4.2. Remove random noise by using LMS Filter

The ideal velocity at each position in space, $d(n)$, was established based on equations (2), (3), and (4). This ideal signal was then added with Gaussian, noise, $v(n)$, which affected the accuracy of the signal. The LMS filter effectively eliminated the impact of Gaussian noise, as shown in Figure 4.

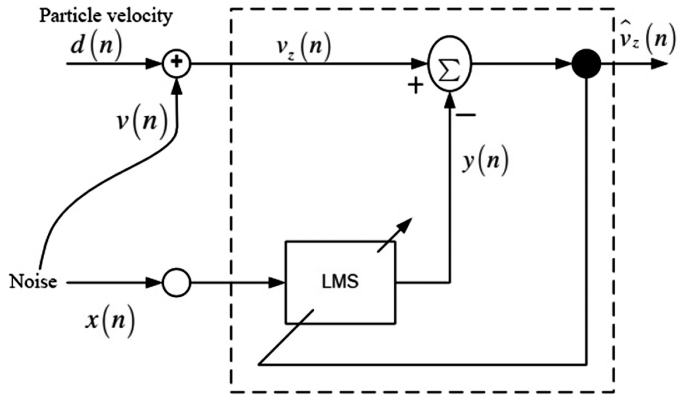

Figure 4. LMS Filter Performance
Reference: The authors

Algorithm 1: Remove Random Noise using LMS Filter

Step 1: Set the step size μ*, the filter length of the LMS filter, and the noise variance.

Step 2: Initialize the coefficients $\omega(n) = 0$.

Step 3: For n=0, 1, 2 …

Calculate the output of the filter. $y(n) = w(n)\, x(n)$

Calculate the prediction error. $e(n) = vz(n) - y(n)$

Update the filter coefficients:

$w(n+1) = w(n) + \mu \times e(n)x(n)$

calculate the filtered signal by convolution.

$$v_z(n) = e(n)$$

Repeat until the end of the signal.

e-ISSN 2357-6014 / Vol. 21, no. 3 / september-december 2025 / Bogotá D.C., Colombia
Universidad Cooperativa de Colombia

4.3. Utilize the AHI algorithm for estimating viscosity and elasticity

We utilized the AHI algorithm to estimate tissue viscosity and elasticity based on shear wave velocity values [9], [15], [18]. The formulas for calculating the elasticity and viscosity of tissue are represented as equations (8) and (9).

$$\mu(x,y) = \Re\left\{\frac{-\rho\omega_0^2 V_z(x,y,\omega_0)}{\nabla^2 V_z(x,y,\omega_0)}\right\} \tag{8}$$

$$\eta(x,y) = \Im\left\{\frac{-\rho\omega_0 V_z(x,y,\omega_0)}{\nabla^2 V_z(x,y,\omega_0)}\right\} \tag{9}$$

$V_z(x, y, \omega_0)$ is determined by applying the Fourier transformation at a specific angular frequency ω_0, and $\nabla^2 V_z(x, y, \omega_0)$ is calculated using the function Discrete Laplacian, represented as $del\,2(V_z(x, y, \omega_0))$, which provides an approximation of the Laplace differential operator applied to $V_z(x, y, \omega_0)$ in discrete form.

4.4. Remove speckle noise by using the median filter

Ultrasound images often contain speckle noise, which can make the images look grainy and less clear, there by affecting the accuracy of medical diagnoses [13][19]. In this research, to reduce speckle noise, a median filter with a window size of 3×3, equivalent to 9 pixels, was employed and precisely positioned at the area requiring filtering in the image. The values of all pixels in the window were arranged in ascending or descending order. Subsequently, the median value, representing the middle position after sorting, was selected. In cases of an even number of pixels, the average of the two middle values was computed. The value at the center of the window, corresponding to the examination area, was then replaced by the selected median value. This process was iterated across all pixels in the image, resulting in noise reduction and the preservation of essential features.

Algorithm 1: Using a median filter to remove the speckle noise

Step 1: Define height and width as the dimensions of the input_image.

Step 2: Iterating over each pixel (i, j) in the input_image:

For i = 2 to (height – 1) do For j = 2 to (width – 1) do

Step 3: Create a 3x3 window around pixel (i, j). Then, extract pixel values within the 3x3 window around pixel (i, j).

Step 4: Sort the values within the window in ascending order.

Step 5: Assign the median value (value in the middle) to the corresponding pixel in output_image.

Step 6: Repeat for all pixels

5. EXPERIMENTAL RESULTS AND DISCUSSION

5.1. Experimental setup

To verify the proposed solution, we set up a simulation scenario as follows. Size of tissue is 80 x 80 mm and digitalized by an image 80 x 80 pixels. Size of tumor is 25 x 25 mm. The viscosity and elasticity values of tissues are shown in Table 1. Density of tissue is 1000 kg/m³. A needle is controlled to vibrate with a vibration frequency of 150 Hz and amplitude of 5 mm. The reflected noise formed at the interface between the two environments (the border between healthy and diseased tissues). Additionally, we added the random noise to simulate actual conditions and explore ways to eliminate this random noise. The amplitude of the reflected and random noises are changed in experimenting.

Table 1. The tissue's elasticity and viscosity

Type of tissue	Elasticity (Pa)	Viscosity (Pa.s)
Healthy tissue	6000	1.2
Disease tissue	7000	1.5

Reference: The authors

5.2. Results analysis

Figure 5 shows the ideal shear wave velocity graph in space, which was simulated by using the FDTD method. It is attenuated-sine shape.

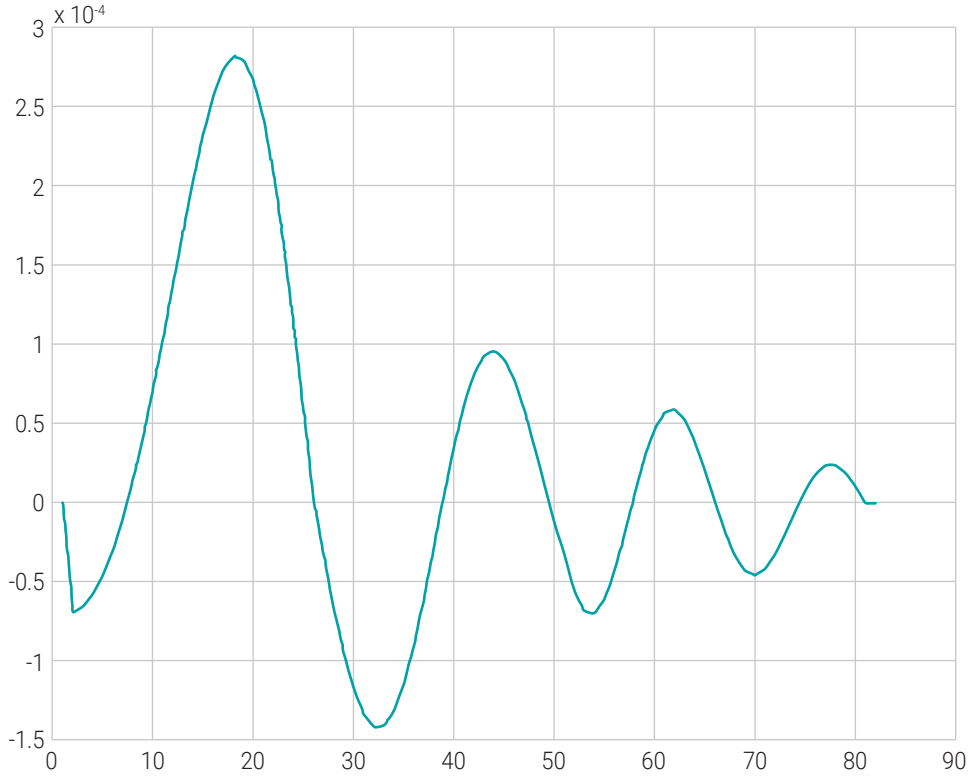

Figure 5. Ideal velocity in space.
Reference: The authors

According simulation scenario, Ideal elasticity and viscosity image are illustrated in the Figures 6a and 6b, respectively.

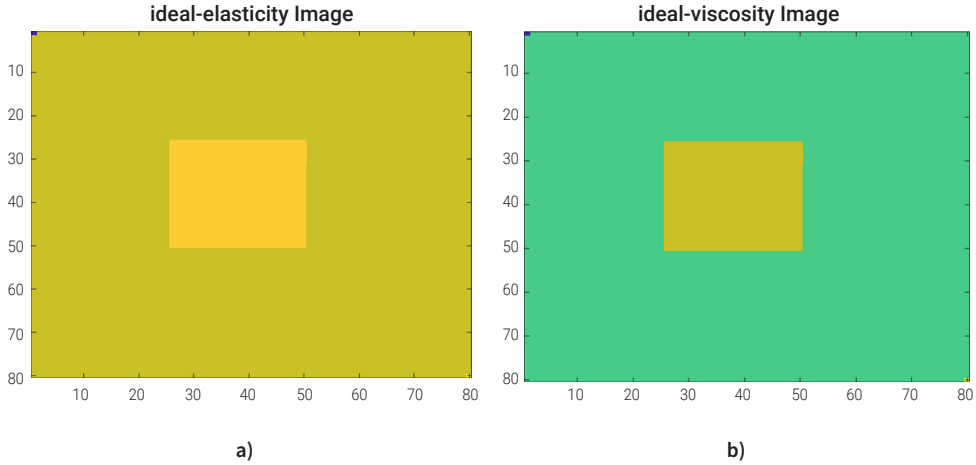

Figure 6. a) Ideal-elasticity image; b) Ideal-viscosity image.
Reference: The authors

After removing reflected and random noises from the shear wave velocity, the estimated elasticity and viscosity images obtained through the application of the AHI algorithm are depicted in Figure 7. The images in Figure 7 are visually comparable to the elasticity and viscosity images in Figure 6. However, there is still some noise in the images, and the contrast is not very high. Noise is more noticeable in the lower-right corner of the images, aligning with the explanation in Figure 8.

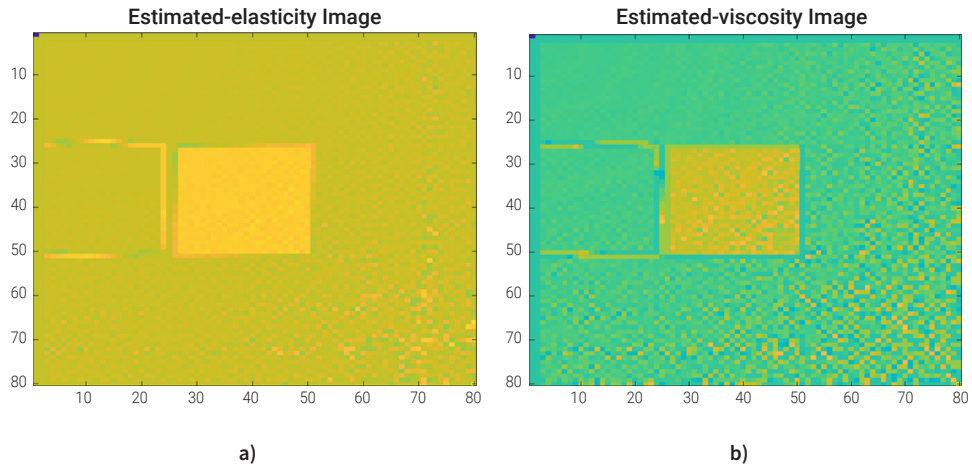

Figure 7. a) Estimated-elasticity image; b) Estimated-viscosity image.
Reference: The authors

To compare the estimated elasticity and viscosity values at each location in space with the ideal elasticity and viscosity values, the author considers a horizontal line with vertical coordinate 30 (line 30), the results are shown in Figure 8. Although some noise remained, the red chart (estimated) closely followed the red chart (ideal). It was noticeable that the estimated-result from the source (position 0) to position 80 in space deteriorates gradually. The reason for this is that the signal-to-noise ratio (SNR) gradually decreases from the source position to positions farther away from the source (shear wave is attenuation sine shape). This observation matched what happened in actual conditions.

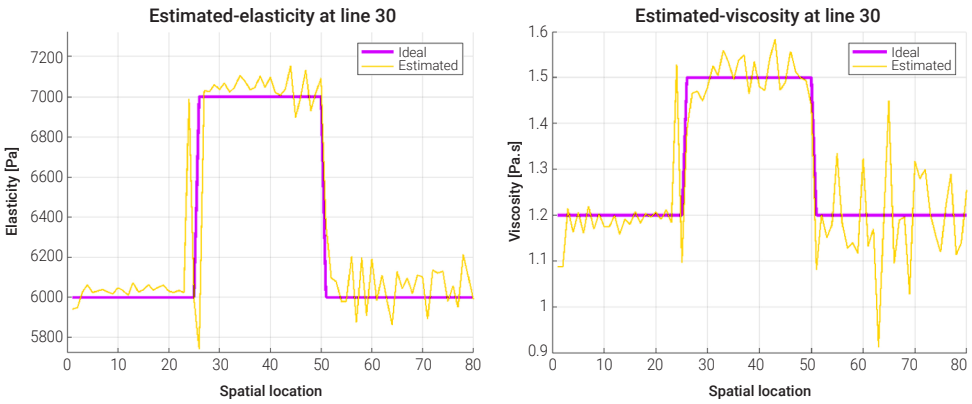

Figure 8. Estimated - elasticity and viscosity at line 30.

A median filter was utilized to remove speckle noise and improve image quality. The results are illustrated in Figure 9. It is evident that the elasticity and viscosity images of the tissue in Figure 9 exhibit improved image quality compared to Figure 7. It can be observed that the noise in Figure 7 has been significantly reduced. These outcomes closely resemble the ideal images compared to before being filtered by the median filter.

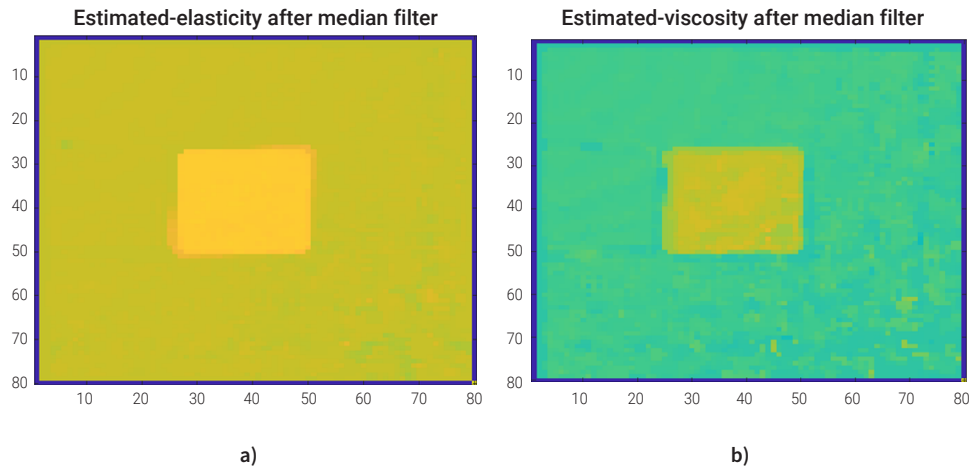

Figure 9. a) Estimated-elasticity image; b) Estimated-viscosity image after using median filter.
Reference: The authors

5.3. Evaluation Measures

Root Mean Square Error (RMSE) is used to measure the magnitude of differences between ideal values and estimated values. Therefore, a smaller ***RMSE*** value indicates

that the estimated value is closer to the ideal value. The Equation (10) is used to calculate the value of $RMSE$.

$$RMSE = \sqrt{\frac{1}{MN}\sum_{i=0}^{M-1}\sum_{j=0}^{N-1}[I(i,j)-K(i,j)]^2} \tag{10}$$

where K is the image before filtering, I is the image after filtering, and MN is the size of the image.

Thus, the $RMSE$ value is effective in evaluating the quality of the proposed solution. However, the calculation of the RMSE value needs to be considered with a specific noise level. Therefore, the signal-to-noise ratio (SNR) is utilized and calculated according to the equation (11). A higher SNR value indicates that the signal intensity exceeds that of the noise. This factor also impacts the resulting estimated elasticity and viscosity images [16-17].

$$SNR = 10 * \log 10\left(\frac{Psignal}{Pnoise}\right) \tag{11}$$

where $Psignal$ is the power of the signal, $Pnoise$ is the power of the noise.

In this study, the RMSE values were calculate with various levels of noises. Specifically, 10 levels of noises were used. For each level of noise, the amplitude of the reflected noise and the random noise were changed. The amplitude of the shear wave remained unchanged at 5 mm.

10 different levels of noise was simulated, and Equation (11) was applied accordingly. Consequently, 10 SNR values ranging from 19.9 dB to 39.9 dB were obtained. In Figure 10, the blue line represents the RMSE values for the estimated - elasticity image before applying median filter, while the red line represents the one after applying median filter. For each SNR value, there is a corresponding RMSE value. It can be observed that the RMSE values after filtering are significantly smaller than before filtering. For example, at the first position where SNR is 19.9, the RMSE value before filtering is 0.13, and the RMSE value after filtering is 0.0639.

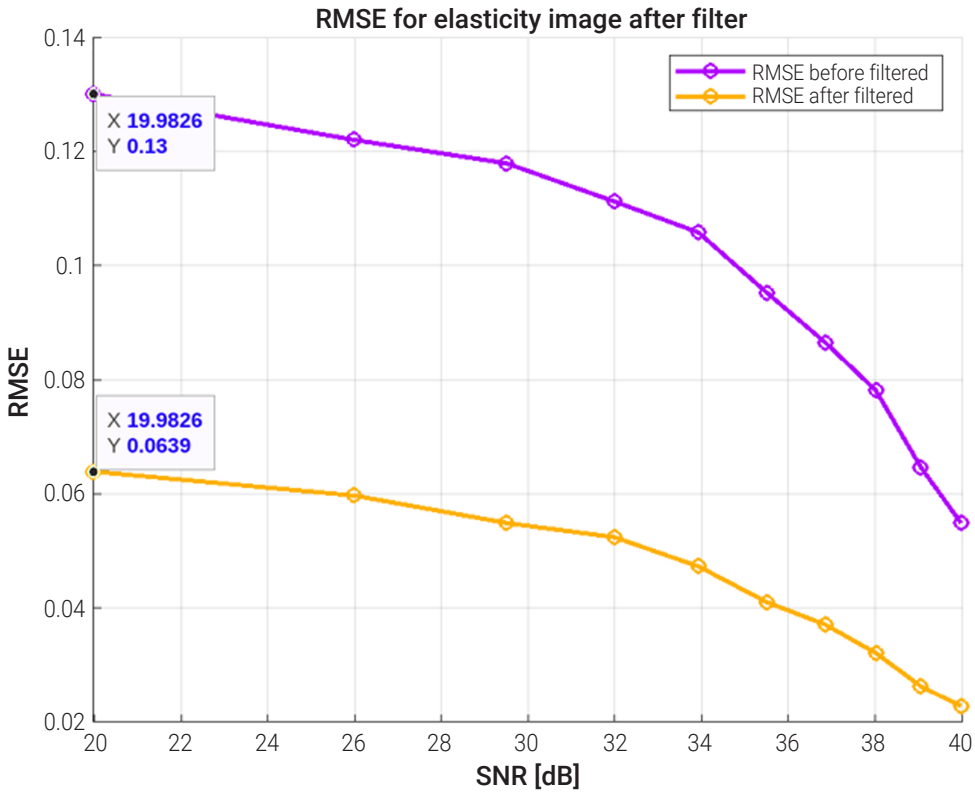

Figure 10. The RMSE values for the estimated - elasticity image corresponding to SNR.
Reference: The authors

In Figure 11, the graph illustrates the RMSE for the estimated - viscosity image before and after applying median filter, similar to Figure 11. The RMSE values for the estimated - viscosity image also decrease significantly after median filtering. From Figures 11 and 12, it can be observed that the RMSE values decrease when the SNR values increase and the RMSE values decrease substantially after applying median filter. This demonstrates the effectiveness of the median filtering method and the influence of SNR to obtained-RMSE values.

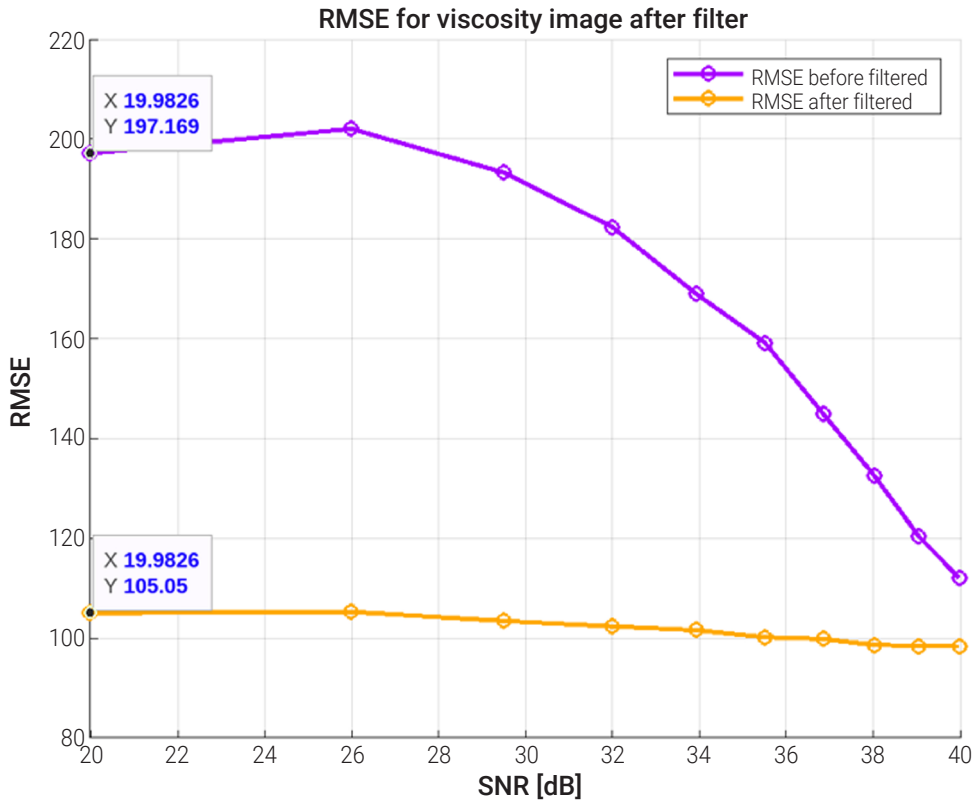

Figure 11. The RMSE values for the estimated - viscosity image corresponding to SNR.
Reference: The authors

6. CONCLUSION AND FUTURE WORK

In this paper, The Finite Difference Time Domain (FDTD) method was utilized to simulate the propagation of shear waves. Next step, effective mitigation of the reflected and random noises was achieved through the utilization of directional filter and LMS filter, respectively. Then the elasticity and viscosity images were estimated successfully by using the AHI algorithm. Finally, a median filter was used to smooth the estimated elasticity and viscosity images. The Root Mean Squared Error standard was used to evaluate the quality of proposed solution.

In the future works, authors will primarily focus on improving the quality of directional filter to completely eliminate reflected noise. Accordingly, enhance the accuracy of the estimation of the elasticity and viscosity images. Additionally, the goal is to develop 3D images for the elasticity and viscosity of tissue, which will facilitate easier tumor detection.

Conflict of interest: There is no conflict of interest to this work.
Funding: Not applicable.

REFERENCES

[1] Shaozhen song, Nhan Minh Le, Zhihong Huang, Tueng Shen, and Ruikang K. Wang, "Quantitative shear-wave optical coherence elastography with a programmable phased array ultrasound as the wave source," Article in Optics Letters. 40, 5007-5010, 2015.

[2] Deffieux T, Gennisson JL, Bercoff J, Tanter M. On the effects of reflected waves in transient shear wave elastography. IEEE Trans Ultrason Ferroelectr Freq Control. 2011 Oct;58(10):2032-5. doi: 10.1109/TUFFC.2011.2052. PMID: 21989866.

[3] Q. H. Luong, S. -H. Nguyen, D. -N. Tran, C. M. Nguyen and D. -T. Tran, "Viscoelastic Estimation of Soft Tissue in the Presence of Gaussian and Reflection Noises Impacting Shear Wave Propagation," 2023 12th International Conference on Control, Automation and Information Sciences (ICCAIS), Hanoi, Vietnam, 2023, pp. 622-627, doi: 10.1109/ICCAIS59597.2023.10382326.

[4] Crosby D, Bhatia S, Brindle KM, Coussens LM, Dive C, Emberton M, Esener S, Fitzgerald RC, Gambhir SS, Kuhn P, Rebbeck TR, Balasubramanian S. Early detection of cancer. Science. 2022 Mar 18;375(6586):eaay9040. doi: 10.1126/science.aay9040. Epub 2022 Mar 18. PMID: 35298272.

[5] Bohunicky B, Mousa SA. Biosensors: the new wave in cancer diagnosis. Nanotechnol Sci Appl. 2010 Dec 30;4:1-10. doi: 10.2147/NSA.S13465. PMID: 24198482; PMCID: PMC3781701.

[6] Chang JM, Moon WK, Cho N, Yi A, Koo HR, Han W, Noh DY, Moon HG, Kim SJ. Clinical application of shear wave elastography (SWE) in the diagnosis of benign and malignant breast diseases. Breast Cancer Res Treat. 2011 Aug;129(1):89-97. doi: 10.1007/s10549-011-1627-7. Epub 2011 Jun 17. PMID: 21681447.

[7] Y. Zheng, S. Chen, W. Tan, R. Kinnick and J. F. Greenleaf, "Detection of tissue harmonic motion induced by ultrasonic radiation force using pulse-echo ultrasound and kalman filter," in IEEE Transactions on Ultrasonics, Ferroelectrics, and Frequency Control, vol. 54, no. 2, pp. 290-300, February 2007, doi: 10.1109/TUFFC.2007.243, 2007.

[8] Zhao, Heng & Qiang, Bo & Amador Carrascal, Carolina & Song, Pengfei & Urban, Matthew & Kinnick, Randall & Greenleaf, James & Chen, Shigao. (2012). Measure Elasticity and Viscosity Using the Out-of-plane Shear Wave. IEEE International Ultrasonics Symposium, IUS. 10.1109/ULTSYM.2012.0053.

[9] Nguyen Sy Hiep, Luong Quang Hai, Tran Duc Nghia, Tran Duc Tan, " Evaluating the Improvement in Shear Wave Speed Estimation Affected by Reflections in Tissue" Intelligent Systems and Networks, Lecture Notes in Networks and Systems (LNNS, volume 752), 2023.

[10] Tran, Duc-Tan & Ha, Nguyen & Luong, Hai & Tran, Duc-Nghia & Shankar, Achyut. (2023). Shear complex modulus imaging utilizing frequency combination in the least mean square/algebraic Helmholtz inversion. Multimedia Tools and Applications. 1-18. 10.1007/s11042-023-17061-7.

[11] S. L. Lipman, N. C. Rouze, M. L. Palmeri and K. R. Nightingale, "Evaluating the Improvement in Shear Wave Speed Image Quality Using Multidimensional Directional Filters in the Presence of Reflection Artifacts," in IEEE Transactions on Ultrasonics, Ferroelectrics, and Frequency Control, vol. 63, no. 8, pp. 1049-1063, Aug. 2016, doi: 10.1109/TUFFC.2016.2558662, 2016.

[12] M. Orescanin, Y. Wang and M. F. Insana, "3-D FDTD simulation of shear waves for evaluation of complex modulus imaging," in IEEE Transactions on Ultrasonics, Ferroelectrics, and Frequency Control, vol. 58, no. 2, pp. 389-398, February 2011, doi: 10.1109/TUFFC.2011.1816, 2011.

[13] Carbente, R.P., Maia, J.M. & Assef, A.A. Image reconstruction utilizing median filtering applied to elastography. BioMed Eng OnLine 18, 22 (2019). https://doi.org/10.1186/s12938-019-0641-6

[14] Garg, Setu & Vijay, Ritu & Urooj, Shabana, "Statistical Approach to Compare Image Denoising Techniques in Medical MR Images". . (2019). Procedia Computer Science. 152. 367-374. 10.1016/j.procs.2019.05.004.

[15] Elira Maksuti, Fabiano Bini, Stefano Fiorentini, Giulia Blasi, Matthew W Urban, Franco Marinozzi and Matilda Larsson, "Influence of wall thickness and diameter on arterial shear wave elastography: a phantom and finite element study" Elira Maksuti et al 2017 Phys. Med. Biol. 62 2694, DOI 10.1088/1361-6560/aa591d

[16] P. Quispe, S. E. Romero and B. Castaneda, "Feasibility of a Deep Learning approach to estimate Shear Wave Speed using the framework of Reverberant Shear Wave Elastography: A numerical simulation study," 2022 44th Annual International Conference of the IEEE Engineering in Medicine & Biology Society (EMBC), Glasgow, Scotland, United Kingdom, 2022, pp. 3895-3898, doi: 10.1109/EMBC48229.2022.9871532.

[17] D. Liu and E. S. Ebbini, "6B-3 Viscoelastic Property Measurement in Thin Tissue Constructs Using Ultrasound," 2007 IEEE Ultrasonics Symposium Proceedings, New York, NY, USA, 2007, pp. 436-439, doi: 10.1109/ULTSYM.2007.118, 2007.

[18] Antonio Callejas, Antonio Gomez, Inas H. Faris, Juan Melchor and Guillermo Rus, " Kelvin–Voigt Parameters Reconstruction of Cervical Tissue-Mimicking Phantoms Using Torsional Wave Elastography." Sensors 2019, 19, 3281; doi:10.3390/s19153281, 2019

[19] T. . Quang Huy, V. . Dung Nguyen, and D. T. . Tran, "The Efficiency of Applying Compressed Sampling and Multi-Resolution Into Ultrasound Tomography", Ing. Solidar, vol. 15, no. 3, pp. 1–16, Sep. 2019, doi: 10.16925/2357-6014.2019.03.08.